

Alexa Griesel · Miguel Angel Morales Maqueda

The relation of meridional pressure gradients to North Atlantic deep water volume transport in an ocean general circulation model

Received: 9 February 2005 / Accepted: 13 December 2005 / Published online: 7 March 2006
© Springer-Verlag 2006

Abstract We use a coarse resolution ocean general circulation model to study the relation between meridional pressure and density gradients in the Southern Ocean and North Atlantic and the Atlantic meridional overturning circulation. In several experiments, we artificially modify the meridional density gradients by applying different magnitudes of the Gent–McWilliams isopycnal eddy diffusion coefficients in the Southern Ocean and in the North Atlantic and investigate the response of the simulated Atlantic meridional overturning to such changes. The simulations are carried out close to the limit of no diapycnal mixing, with a very small explicit vertical diffusivity and a tracer advection scheme with very low implicit diffusivities. Our results reveal that changes in eddy diffusivities in the North Atlantic affect the maximum of the Atlantic meridional overturning, but not the outflow of North Atlantic Deep Water into the Southern Ocean. In contrast, changes in eddy diffusivities in the Southern Ocean affect both the South Atlantic outflow of North Atlantic Deep Water and the maximum of the Atlantic meridional overturning. Results from these experiments are used to investi-

gate the relation between meridional pressure gradients and the components of the Atlantic meridional overturning. Pressure gradients and overturning are found to be linearly related. We show that, in our simulations, zonally averaged deep pressure gradients are very weak between 20°S and about 30°N and that between 30°N and 60°N the zonally averaged pressure grows approximately linearly with latitude. This pressure difference balances a westward geostrophic flow at 30–40°N that feeds the southbound deep Atlantic western boundary current. We extend our analysis to a large variety of experiments in which surface freshwater forcing, vertical mixing and winds are modified. In all experiments, the pycnocline depth, assumed to be the relevant vertical scale for the northward volume transport in the Atlantic, is found to be approximately constant, at least within the coarse vertical resolution of the model. The model behaviour hence cannot directly be related to conceptual models in which changes in the pycnocline depth determine the strength of Atlantic meridional flow, and seems conceptually closer to Stommel's box model. In all our simulations, the Atlantic overturning seems to be mainly driven by Southern Ocean westerlies. However, the actual strength of the Atlantic meridional overturning is not determined solely by the Southern Ocean wind stress but as well by the density/pressure gradients created between the deep water formation regions in the North Atlantic and the inflow/outflow region in the South Atlantic.

A. Griesel
Potsdam Institute for Climate Impact Research,
Telegraphenberg, 14473 Potsdam, Germany

Present address: A. Griesel (✉)
Scripps Institution of Oceanography,
233 Nierenberg Hall, La Jolla,
CA 92093-0230,
USA
E-mail: agriesel@ucsd.edu
Tel.: +1-858-8224325
Fax: +1-858-5349820

M. A. M. Maqueda
Center for Atmosphere Ocean Science,
Courant Institute of Mathematical Sciences,
New York University, New York, NY USA

Present address: M. A. M. Maqueda
Proudman Oceanographic Laboratory,
Liverpool, UK

1 Introduction

For many years a discussion has evolved around the issue of what determines the strength of the Atlantic meridional overturning circulation (MOC). The prevailing picture is that of a circulation driven by diapycnal mixing in the ocean interior and, perhaps,

controlled by the volume rate of formation of North Atlantic deep water (NADW) (Munk and Wunsch 1998; Huang 1999; Wunsch and Ferrari 2004). Within this conceptual framework, downward turbulent diffusion of heat at low latitudes is balanced by upwelling of deep water. This upward transport of water is compensated by high-latitude downwelling associated with deep ocean convection in the North Atlantic. According to this theory, the strength of the Atlantic MOC is then determined by the amount of energy involved in the vertical mixing of heat, this energy being ultimately provided by winds and tides.

An alternative description of the Atlantic MOC has been suggested by Toggweiler and Samuels (1993a), Toggweiler and Samuels (1995) and Toggweiler and Samuels (1998) in which the sinking of NADW is identified as the closing branch of a circulation driven by wind-driven upwelling in the Southern Ocean. Waters at the surface of the Southern Ocean move northward as a result of strong Ekman drift caused by circumpolar winds and are returned at depths below that of the sill of Drake Passage. This “Drake Passage effect” is explained by the fact that no net zonal pressure gradient can be created at the latitude of Drake Passage above the depth of its sill and, accordingly, no net meridional geostrophic flow can exist at shallower depths. Within this framework, the strength of the Atlantic MOC would be determined solely by the strength of the upwelling caused by the dominant westerlies in the Southern Ocean.

The mechanism presented by Toggweiler and Samuels (1993a) has received further theoretical support in a recent work by Nof (2003). Nof (2003) considered the net momentum balance of a water column from the surface down to the depth of the sill of Drake Passage. In order to cancel out the effects of pressure, Nof (2003) calculated the integral of such balance along a closed contour passing through the tips of the Americas, Africa and Australia. As it turns out, this integral provides a direct relation between the wind stress along the contour and the meridional transport across it, showing therefore that the net inflow into the Atlantic, Indian and Pacific oceans above the sill of Drake Passage is uniquely determined by the surface wind. According to Nof's estimate, 9 ± 5 Sv cross his contour into the Atlantic, marking the starting point of the northbound branch of the Atlantic MOC. An important point stressed by Nof (2003) is that the flow in this branch is partitioned between a northbound Sverdrup transport in the ocean interior and a southbound western boundary current flow. Hence, ocean pressure gradients need to somehow adapt so that the Sverdrup flow minus the western boundary flow equals the northbound Ekman transport, a result that highlights the importance of the interaction between the wind-driven and thermohaline-driven components of the circulation. However, regardless of the nature of such interaction, changes in the pressure gradients will not affect the net northward transport. If one then assumes, as Nof (2003) does, a

partitioning of the wind-driven transport between the Indopacific and the Atlantic proportional to the widths of the respective basins along the integration contour, then the conclusion that the Atlantic inflow and outflow cannot be affected by alterations in the zonal and meridional pressure gradients seems inescapable.

In this paper, we put this conclusion to the test by running a series of experiments with a global coarse-resolution ocean model in which changes in pressure gradients are caused by varying the strength and geographical distribution of the diffusion coefficients of the parameterized baroclinic eddy transport.

More specifically, we show in the first part of the paper how changes in the density gradients in the Southern Ocean and North Atlantic affect on the one hand the water inflow into the Southern Ocean and the deep water formation in the North Atlantic on the other hand. To do so, we force modifications in the density gradients by changing the magnitude of the eddy thickness diffusivity (Gent and McWilliams 1990) in different regions of the ocean. Note that our focus here is not on how the representation of baroclinic eddies affects the simulated ocean circulation, but, in a more conceptual way, on how changing the density gradients in different regions of the ocean may change the volume transports. Kamenkovich and Sarachik (2004) have recently reported on experiments with a similar design, and our work largely confirms, as well as extends, their findings. As in Kamenkovich and Sarachik (2004), our experiments show that changing eddy diffusivities, and hence density gradients, in the North Atlantic significantly affects the upwelling within the Atlantic but has little impact on the South Atlantic outflow, whereas changing eddy diffusivities in the Southern Ocean has the biggest impact on the South Atlantic outflow. However, in contrast to Kamenkovich and Sarachik (2004), we investigate the resulting changes in volume transport in a parametric regime that is very close to the limit of no diapycnal mixing. In our model, strictly horizontal diffusion is negligible, as the model operates with zero explicit horizontal diffusivity, the implicit diffusion caused by the numerical advection scheme (Prather 1986) is very low, and vertical diffusivities ($0.05 \times 10^{-4} \text{ m}^2 \text{ s}^{-1}$) are much smaller than commonly used. We show that even without horizontal diffusion and its associated Veronis effect (Lazar et al. 1999), there is a significant amount of upwelling and meridional recirculation in the North Atlantic that is affected by the strength of the eddy diffusivities, and that it is therefore important to clearly distinguish between the maximum of the Atlantic MOC and the South Atlantic outflow (the difference between the two being equal to the recirculation within the Atlantic) even in an ocean close to the limit of no diapycnal mixing and hence with little upwelling driven by downward heat diffusion.

In the second part of the paper, we investigate the quantitative relation between meridional pressure gradients and the meridional volume transport in the model. Many authors have used OGCMs to show

diagnostically that there seems to be a linear relation between the strength of the MOC and hemispheric or inter-hemispheric meridional gradients of the zonally averaged pressure or density (see Rahmstorf 1996, and references therein). The relation of meridional pressure gradients to the MOC also is particularly relevant for zonally averaged models, where it is often postulated that the east-west density difference can be expressed in terms of the zonally averaged meridional density difference (see e.g. Wright et al. 1997 and references therein). We show that deep meridional pressure gradients in the Atlantic (below about 1,000 m) are very weak south of about 40°N and that the maximum of the Atlantic MOC is very well correlated with the deep pressure gradient between 40°N and 60°N. This North-South pressure gradient creates a westward geostrophic flow that is ultimately collected along the eastern flank of North America. Part of this flow wells up in the area of the Grand Banks and the remaining part flows southward in a deep western boundary current. The linear relation between deep meridional pressure gradient and meridional volume transport is robust and holds for all our experiments, which include a large variety of changes in the surface forcing and the horizontal and vertical mixing coefficients. We also examine the dependence of the maximum of the Atlantic MOC and the South Atlantic outflow on the meridional pressure and density gradients calculated within the pycnocline, above the mean level of no motion (located at about 1,000 m). A linear relation between the strength of the Atlantic MOC and the meridional pressure gradient exists in the pycnocline but is somewhat less robust. A key feature of our simulations is that, contrary to classical scaling laws that relate the depth of the pycnocline to the strength of the Atlantic MOC, the depth of the pycnocline is only weakly responsive to changes in the maximum of the Atlantic MOC or the South Atlantic outflow.

The paper is organized as follows. The first section describes the model and its standard configuration near the limit of no diapycnal mixing. The second section describes the outcome of experiments where the eddy diffusion coefficient is changed in the North Atlantic and Southern oceans. The third section investigates the relation between meridional pressure gradients and the maximum of the MOC. The fourth section describes a conceptual model for the relation between pressure gradients and volume transport under constant wind forcing and critically assesses Nof's hypotheses. The fifth section extends the analysis of the two previous sections to a variety of experiments, including increased vertical mixing and different surface forcing and winds.

2 Model

The ocean model used is based on the GFDL MOM3, coupled to a simple moisture balance model, with

atmospheric fluxes calculated from bulk formulae. Absorbed shortwave radiation is calculated as in Zillmann (1972) over open water and as in Shine (1984) over sea ice. Net surface longwave radiation is parameterized following Berliand and Berliand (1952). Turbulent heat and momentum fluxes formulations are those of Large and Pond (1981) and Large and Pond (1982) over the ocean and of Parkinson and Washington (1979) over sea ice. The surface air temperatures, specific humidities and winds needed for these calculations are derived from long-term monthly mean climatologies calculated from NCEP reanalysis fields (Kalnay et al. 1996). However, the humidity climatology is not directly used in the flux calculations. Rather, the effective specific humidities consist of the climatological values plus an anomaly term that accounts for the modelled water vapor transfer between the atmosphere and the ocean and its subsequent horizontal transport. In this way, the model exactly conserves water. The river runoff is diagnosed from a restoring to sea surface salinity at coastlines whenever the implied freshwater flux is into the ocean. No restoring to salinity elsewhere needs to be applied. The model includes the dynamic thermodynamic sea-ice model described by Fichefet and Maqueda (1997), with the only major difference that now ice dynamics is calculated using an elastic-viscous-plastic rheology. The ocean model has a nonlinear explicit free surface and incorporates a second order moments polynomial advection scheme for tracers (Prather 1986). This advection scheme has associated numerical diffusivities much weaker than more conventional advection schemes (Hofmann and Morales-Maqueda 2006), and so it can be claimed that the effective vertical diffusivity in the model is only the explicit one. The horizontal resolution is 4°× 4° with 24 vertical variably spaced levels ranging from 25 m thickness at the surface to ca. 500 m at depth (see Table 1). The topography is based on the 1/12° ETOPO5 dataset (National Geophysical Data Center 1988). Due to the coarse horizontal resolution, the Bering Strait is kept closed but the model allows for crossland mixing of temperature and salinity (Pacanowski and Griffies 1999).

Table 1 Depths of tracer and velocity grid points and corresponding resolutions

Level	Depth (m)	Δz (m)	Level	Depth (m)	Δz (m)
1	12.50	25	13	876.81	212.98
2	37.50	25	14	1,108.48	250.83
3	62.50	25	15	1,378.48	289.16
4	87.50	25	16	1,686.81	327.01
5	112.50	26.50	17	2,032.52	336.46
6	140.54	32.50	18	2,413.75	397.46
7	177.50	44.34	19	2,827.76	428.62
8	229.21	61.74	20	3,271.00	455.72
9	301.00	84.27	21	3,739.21	478.25
10	397.76	111.37	22	4,227.50	478.25
11	523.75	142.38	23	4,730.51	507.49
12	682.52	176.53	24	5,242.50	513.49

The horizontal viscosity is $3.5 \times 10^5 \text{ m}^2 \text{ s}^{-1}$ at the equator and is tapered with the cosine of the latitude to guarantee numerical stability in high latitudes. In this way, the Munk boundary layer is resolved with at least one grid point at all latitudes. A constant vertical viscosity of $10 \times 10^{-4} \text{ m}^2 \text{ s}^{-1}$ is applied. Our baseline configuration prescribes a constant very low diapycnal diffusion coefficient of $0.05 \times 10^{-4} \text{ m}^2 \text{ s}^{-1}$ and an isopycnal diffusion coefficient of $2,000 \text{ m}^2 \text{ s}^{-1}$. For the representation of eddy transport we use the skew flux approach for the Gent–McWilliams parameterization (Griffies 1997), with a constant coefficient of $100 \text{ m}^2 \text{ s}^{-1}$. No horizontal background diffusivity is applied in any run. The tracer timestep is 1/2 day.

Figure 1 shows the Atlantic overturning streamfunction (left panel) and the Atlantic upwelling at a depth of ca. 1,000 m in Sv (right panel) for the baseline configuration (STD) after an integration of 4,050 years. We note that, even with a vertical mixing coefficient of only $0.05 \times 10^{-4} \text{ m}^2 \text{ s}^{-1}$, the maximum of the Atlantic overturning is around 19 Sv and the South Atlantic outflow amounts to 11 Sv. Upwelling of NADW takes place mainly in the Southern Ocean, with the exception of a small recirculation cell of 8 Sv within the North Atlantic between latitudes of 35–50°N. The upwelling/recirculating areas in the North Atlantic shown in red in Fig. 1 occur predominantly along the western boundary at latitudes where the flow at depths above 1,000 m detaches from the coast and turns eastward while the flow below 1,000 m turns westward into the western boundary current. The zonal integral of the meridional currents at 1,000 m is almost zero at all latitudes inside the Atlantic. Below, we will refer to this level where the net meridional volume transport is zero as the ‘level of no mean motion’.

We stress that this localized upwelling occurs in spite of the very low horizontal and vertical diapycnal mixing in our model. Veronis (1975) attributed this type of

upwelling to spurious horizontal diffusion at steeply sloping isotherms in the western boundary current (the so called Veronis effect). The inclusion of isopycnal eddy stirring and thickness diffusion was seen to indeed partly remove this kind of upwelling (Böning et al. 1995; Lazar et al. 1999). Huck et al. (1998) argued, that the upwelling along the boundaries is not only the consequence of horizontal diffusion but also depends on the formulation of momentum dissipation. They show that Laplacian friction with a no-slip boundary condition generates large vertical diapycnal transports at lateral boundaries whereas a formulation with Rayleigh friction and no-normal-flow boundary conditions reduces the upwelling.

Yang (2003) argued that spurious upwelling along the boundaries could be the result of a poorly resolved western boundary layer. In our model configuration, the western boundary layer is only ‘resolved’ by one grid point and the horizontal scale for dissipating the vorticity imposed by the wind stress curl is therefore prescribed. As discussed by Yang (2003), this could indeed be leading to spurious horizontal flow convergences and divergences in our simulations. We will see in the next section that with higher Gent–McWilliams eddy coefficients in the North Atlantic, the boundary upwelling is in fact reduced.

3 Eddy diffusivities in the North Atlantic and Southern Ocean and their influence on the Atlantic outflow and maximum overturning

In this section we discuss experiments where we apply different magnitudes of the Gent–McWilliams (GM) eddy coefficient in different parts of the model domain. Specifically, in each simulation we increase the GM eddy diffusivities in only one of the following regions: (1) the Southern Ocean, south of 40°S (SO), (2) the

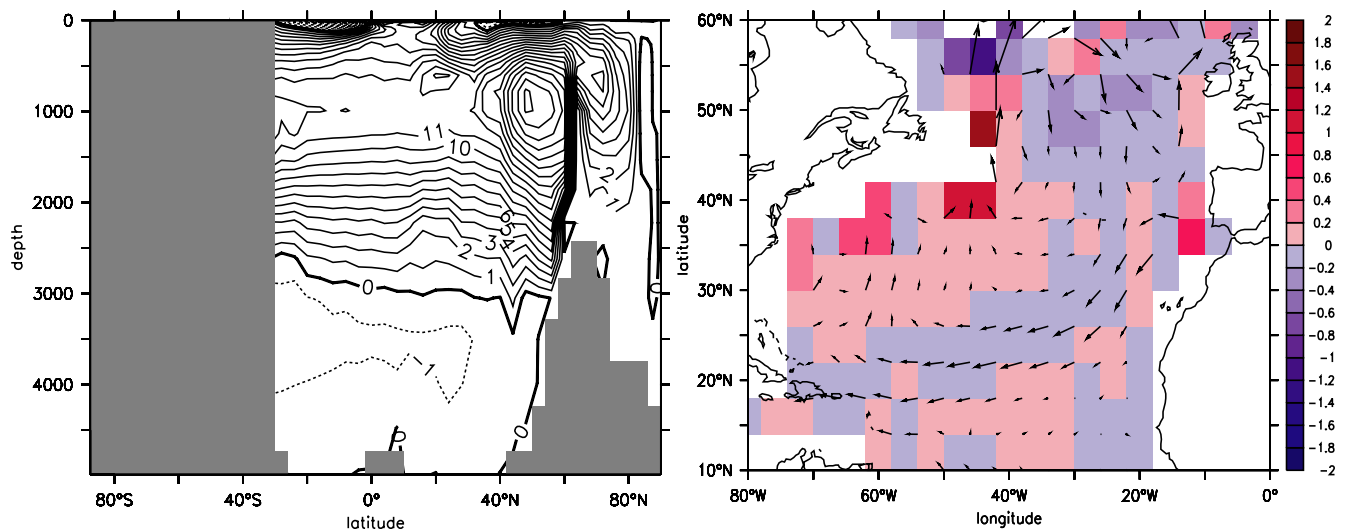


Fig. 1 Standard configuration, with $\kappa_v = 0.05 \times 10^{-4} \text{ m}^2 \text{ s}^{-1}$. Left Atlantic overturning streamfunction. Contour interval is 1 Sv. Right Upwelling in Sv (red) and horizontal currents at 1,000 m in the Atlantic between 10°N and 60°N

high-latitude North Atlantic and Arctic, north of 60°N (NA), and (3) in the low and mid-latitude North Atlantic, between the equator and 60°N (TROPNA), while elsewhere the thickness diffusivities are kept at their baseline value ($100\text{ m}^2\text{ s}^{-1}$). For each region, we conduct five simulations in which the eddy coefficients are increased by 250, 500, 1,000, 2,000 and $2,500\text{ m}^2\text{ s}^{-1}$. The following notations are used: MAXA for the maximum Atlantic overturning, SAO for South Atlantic outflow of NADW at 30°S , $\text{AUP} = \text{MAXA} - \text{SAO}$ for the strength of the upwelling within the Atlantic Ocean, GIN for the southward overflow from the Greenland–Iceland–Norwegian Seas, and IRM for the sinking south of the Denmark Strait sill close to Irminger Sea. All these experiments use as initial conditions the ocean state of year 4,050 of the control simulation. The experiments are labeled with their corresponding symbol (SO, NA, or TROPNA) followed by the magnitude of the change in the GM coefficients. For example, experiment SO1000 is the experiment in which the GM coefficient was increased by $1,000\text{ m}^2\text{ s}^{-1}$ south of 40°S .

Figure 2 displays time series of the different volume transport components of the Atlantic overturning for the simulations SO1000 and NA1000. In both experiments, the maximum Atlantic overturning decreases with respect to that of the control run. However, the decrease is more drastic in SO1000. In the SO1000 experiment, eddies act immediately to reduce the surface water inflow into the Atlantic, while the maximum overturning and deep water formation are not initially reduced as much. As a consequence, there is a significant increase in North Atlantic upwelling during the first 100 years of the experiment. It then takes another 800 years to reach a new equilibrium in which deep water formation rates have adapted to the decreased South Atlantic inflow and outflow. In the NA1000 experiment, there is an initial decrease in all variables, the equilibrium state, however, shows a decrease in the maximum Atlantic overturning of only 3 Sv, a decrease

that is mainly due to a reduction in IRM sinking. Six hundred years after the initial shake, the South Atlantic outflow goes back to its original strength. Figure 3 displays the differences of the Atlantic meridional streamfunction between the SO1000, NA1000 and TROPNA1000 experiments and the control run. When enhanced eddy mixing is applied south of 40°S (SO1000), both the South Atlantic outflow and the upwelling within the Atlantic considerably decrease. In contrast, for experiments with increased diffusivities in the North Atlantic (NA1000 and TROPNA1000), significant changes occur only north of 40°N , where the meridional recirculation and deep water formation occur.

We investigate now the relative changes in meridional transport quantities as the GM coefficients are varied. In addition to the experiments cited above, we include here as well a set of experiments in which the coefficients were increased by up to $2,500\text{ m}^2\text{ s}^{-1}$. Figure 4 shows the maximum of the Atlantic overturning, the South Atlantic outflow, the GIN Seas overflow and the the Irminger Sea downflow from the equilibrium solutions of the SO, NA and TROPNA runs. Of particular interest is that, in the experiments where the GM coefficient was changed only in the North Atlantic, the South Atlantic outflow does not noticeably change (Fig. 4 top-right panel). In these experiments, it is only the upwelling within the Atlantic that decreases with increasing GM coefficient. For all experiments, the GIN Seas sinking only slightly decreases and, therefore, the decrease in the maximum of the Atlantic overturning can be mainly attributed to a decrease in the sinking south of the sills (Fig. 4 bottom-left and bottom-right, respectively). Note as well that a plateau is reached for the SO runs such that, for sufficiently large GM coefficients, the maximum of the Atlantic overturning and South Atlantic outflow are not reduced any further. On the other hand, for coefficients of $2,000\text{ m}^2\text{ s}^{-1}$ or larger in the North Atlantic, the overturning is completely

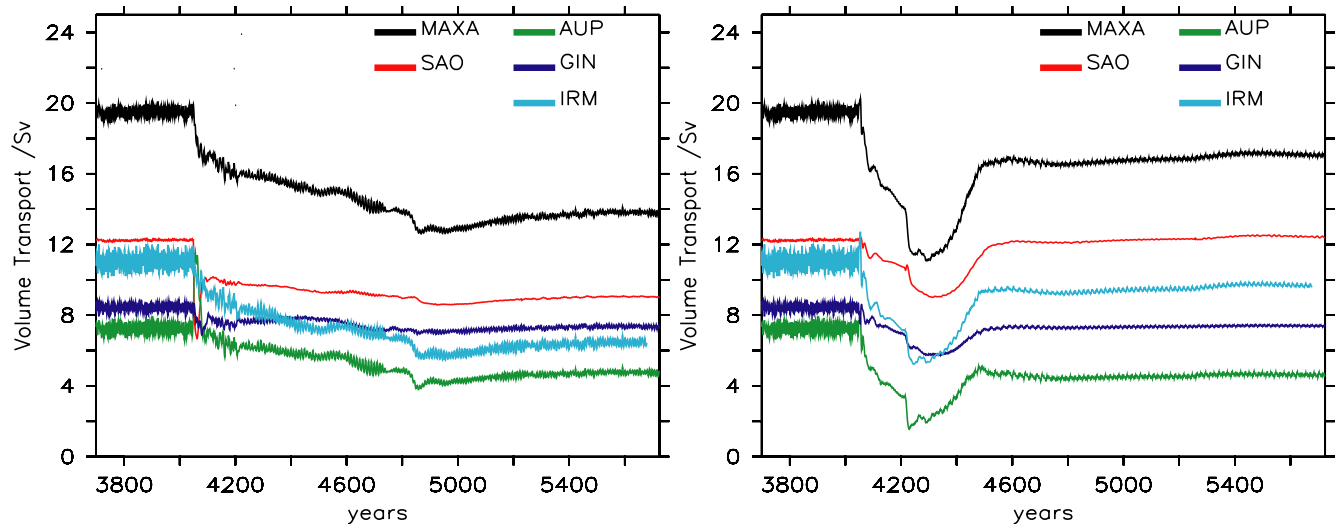


Fig. 2 Time series of ‘switch-on’ experiments. *Left* SO1000. *Right* NA1000. The switch to higher eddy coefficients occurred in year 4,050

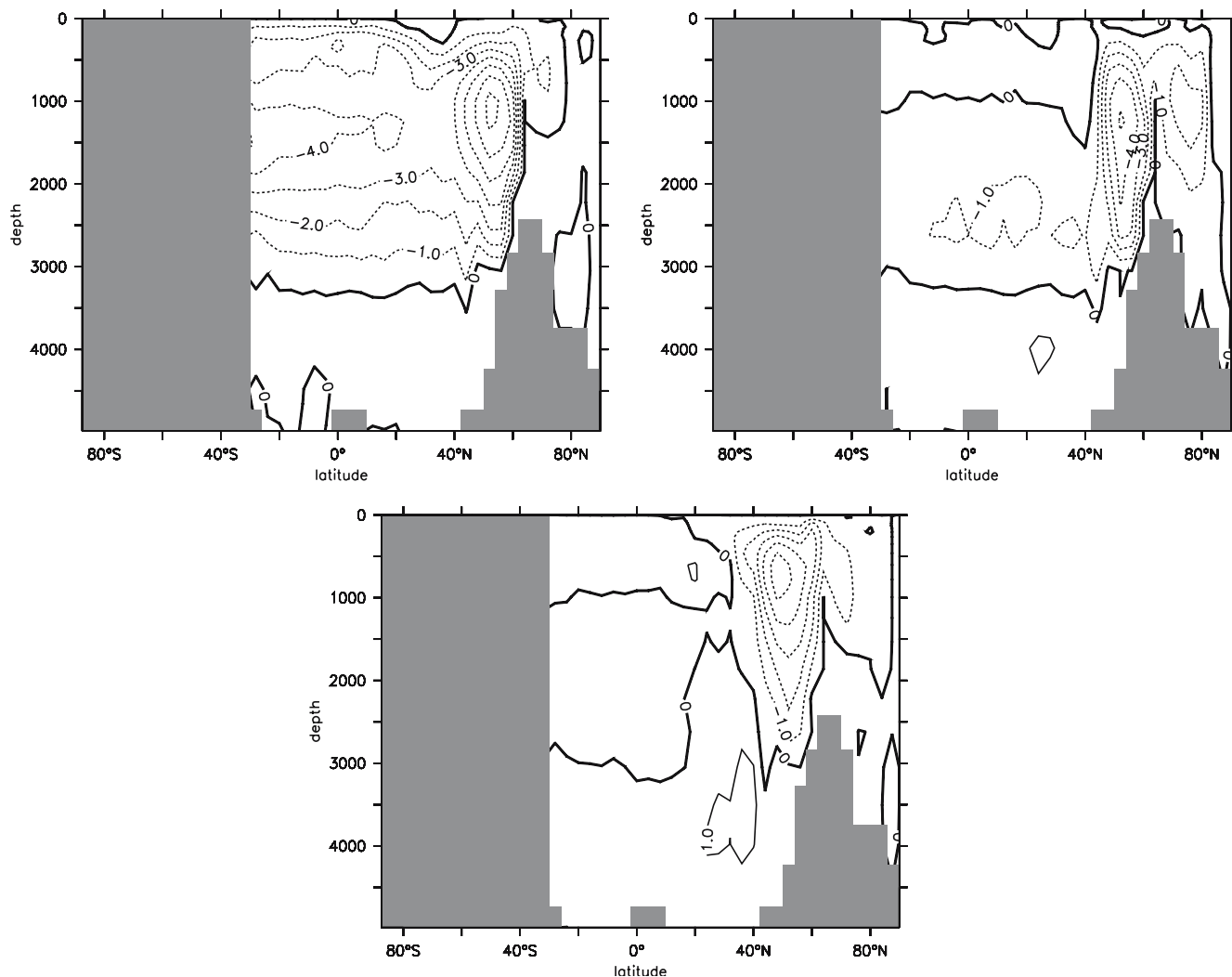


Fig. 3 Atlantic overturning streamfunction differences. *Upper left* SO1000-STD. *Upper right* NA1000-STD. *Lower panel* TROPNA1000-STD. Contour interval is 1 Sv

killed (not shown). To get an estimate of how large the contribution of the SAO is to the maximum overturning, Fig. 5 shows the ratio of the South Atlantic outflow to the maximum overturning, that can be interpreted as a kind of interhemispheric transport efficiency. A ratio of 1 implies that all the waters that sink in the IRM and GIN Seas are exported to the Southern Ocean, and a ratio of 0 means that all the deep water formed in the North Atlantic wells up within the Atlantic. In all the SO experiments, the ratio is constant at ca. 0.6 (left panel of Fig. 5). Since the South Atlantic outflow decreases with increasing GM coefficients, the upwelling within the Atlantic adapts to these changes in such a way that the SAO is always 60% of the maximum overturning. This is an interesting aspect and probably has to do with the origin of the spurious upwelling within the North Atlantic ocean. This upwelling could be the result of spurious convergences and divergences of the horizontal flow due to the poor resolution of the boundary layer (Yang 2003) and hence directly related to the strength of

the horizontal flow made up by SAO. In the NA experiments on the other hand, the ratio increases with increasing GM coefficient since, in these experiments, the upwelling within the Atlantic decreases, while the South Atlantic outflow stays the same. A flattening of isopycnals with increasing GM coefficient in the polar front region of the North Atlantic leads to weaker vertical velocity shears and weaker horizontal recirculations and upwelling.

We stress here again, that, in our simulations, changes in the upwelling and meridional recirculation within the Atlantic are unlikely to be related to changes in the rate of diapycnal mixing. Upwelling in the Atlantic interior driven by vertical diapycnal diffusion ($\kappa_v = 0.05 \text{ cm}^2 \text{ s}^{-1}$) can be estimated by assuming a balance between diapycnal diffusive transport and vertical advection:

$$W_{ad} = \kappa_v \int \int \frac{\partial_{zz}\rho}{\partial_z\rho} dx dy,$$

Fig. 4 Equilibrium volume transports as a function of enhanced eddy diffusivity for SO (black), NA (red) and TROPNA (green) runs. *Top left a* Maximum Atlantic overturning. *Top right b* South Atlantic outflow. *Lower left c* GIN Seas sinking. *Lower right d* sinking south of the Denmark Strait sill

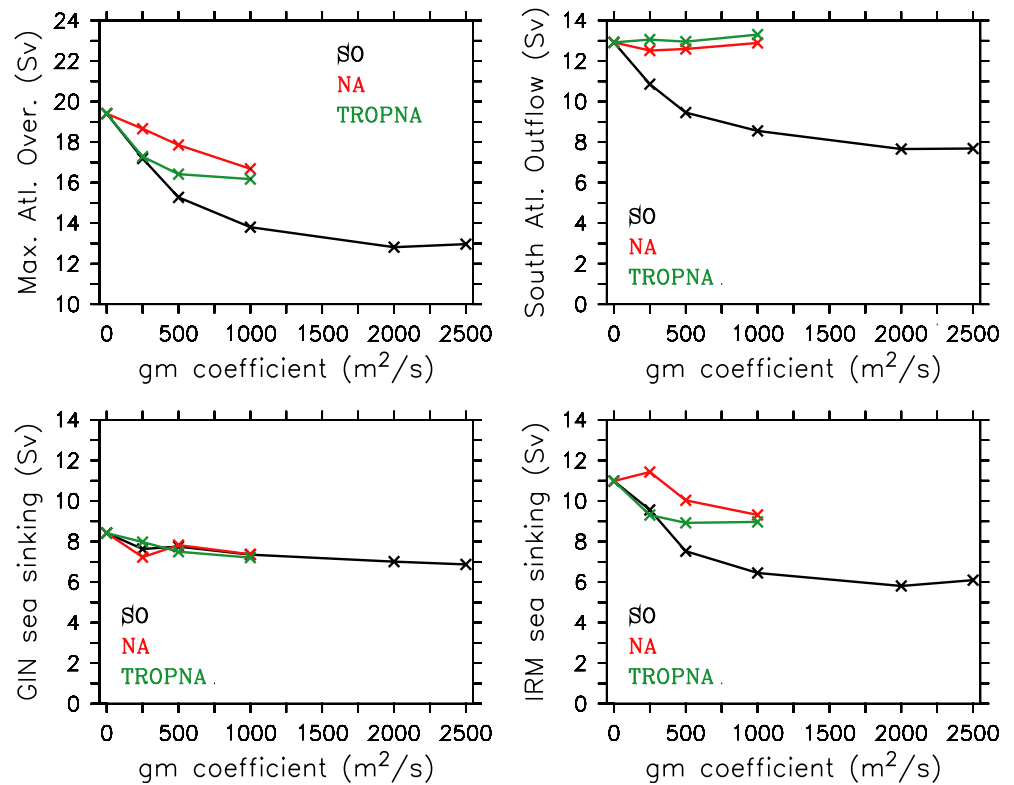
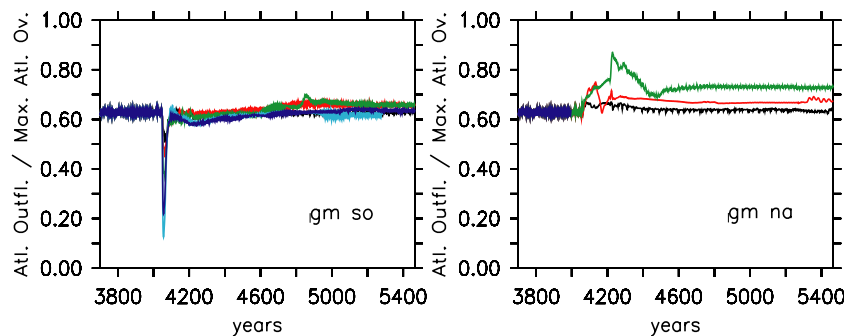


Fig. 5 Ratio of South Atlantic outflow to maximum Atlantic overturning for SO (left) and NA (right) runs; black SO250 and NA250, red SO500 and NA500, green SO1000 and NA1000, blue SO2000 (zero Atlantic overturning for NA), light blue SO2500 (zero Atlantic overturning for NA)



where W_{ad} is the horizontal integral of the vertical velocity at the depth of the MAXA calculated between 30°S and the latitude at which the MAXA occurs. In all our experiments, W_{ad} is relatively constant and below 0.5 Sv. Hence, changes in Atlantic upwelling cannot be attributed in our model to changes in the diapycnal diffusion driven upwelling nor, in principle, to changes in the Veronis effect.

The results described in this section are similar to those reported by Kamenkovich and Sarachik (2004), who obtained a larger response of the Atlantic overturning to variations in eddy diffusion in the Southern Ocean than in the North Atlantic. However, they attribute the changes in their modeled North Atlantic to a decrease in the Veronis effect due to the switch from horizontal to isopycnal diffusion. We have shown however here that increasing GM diffusivities north of 60°N, away from the upwelling regions, in the NA

experiments also leads to a decrease in the overturning. We have not investigated the nature of this model behaviour in detail, but we observe in the model that higher GM coefficients in the GIN Seas tend to weaken the west-east density contrast at the surface between the waters of the East Greenland Current and those of the Norwegian Current. The relatively fresh waters of the East Greenland current extend further east than in the control run, thus decreasing the density of the sinking waters. Although the volume of GIN Seas deep water formation only slightly decreases (Fig. 4, bottom left), the density of the waters overflowing the sills diminishes substantially, as shown in Fig. 6. The decreased density of the overflowing waters leads then to a weaker meridional density gradient between 40°N and 60°N and a reduction both of the sinking in the Irminger Sea and the upwelling within the Atlantic. For eddy coefficients higher than 2,000 m² s⁻¹, this

decrease in density causes the cessation of the entire Atlantic overturning.

Changes in density and pressure gradients caused by the modification of the GM coefficients must ultimately be responsible for the changes in the Atlantic meridional overturning. We explore in the next section how the volume transports are related to meridional pressure differences in the model.

4 The relation of volume transport to meridional pressure gradients

In this section we investigate the dependence of the Atlantic MOC on north–south pressure differences. By increasing the GM coefficient in different regions of the model domain, we decrease the corresponding horizontal density gradients and, accordingly, the pressure differences. We aim in this way at determining whether the meridional gradients of density and pressure can be unambiguously related to the maximum of the Atlantic MOC and the South Atlantic volume outflow. In Sect. 4.1, we identify a specific meridional pressure difference that correlates optimally with the strength of the MAXA and explain this linear relation as a result of geostrophic dynamics. Section 4.2 describes the relation between the MOC and baroclinic and barotropic pressure components at different depths.

4.1 Linear relation with meridional vertically integrated pressure difference

The dynamically most relevant variable for the maximum of the Atlantic overturning is the pressure vertically integrated over the ocean layers above and below the level of no mean motion. For all experiments, the level of no mean motion, as given by the depth at which the zonally integrated volume transport changes from northbound to southbound, is located at a depth of about 1,000 m. The upper panels of Fig. 7 display the

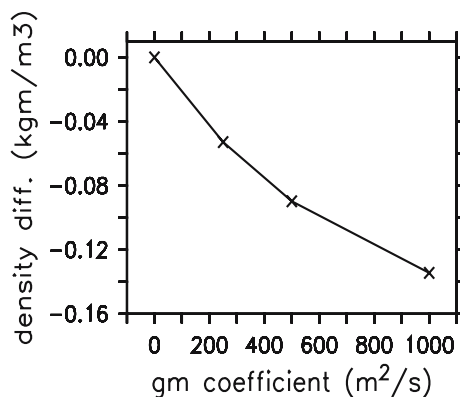


Fig. 6 Averaged density of the waters overflowing the sills from the GIN Seas minus the corresponding density of the baseline model configuration as a function of the GM coefficient in the GIN Seas

flow and pressure integrated over the upper and lower layers, respectively, for the standard configuration. The interesting aspect about these two pressure distributions is that, whereas the surface gyre circulations are apparent in the integral over the upper layer (left panel of Fig. 7), the pressure is relatively uniform between about 40°N and 40°S for the lower layer in the right panel of Fig. 7. Both in the upper and lower layers, the absolute pressure minimum is located in the area of the Antarctic Divergence. For the lower layer, in the North Atlantic, the flow of NADW turns west zonally into the western boundary of the Atlantic at around 40°N, and then evolves as a deep western boundary current until it joins the ACC. Ocean interior circulations are negligible compared to the strength of the deep western boundary current. The dynamically important pressure difference for the deep layer is between the high pressure north of 40°N (where the dense water masses formed in the Nordic Seas and South of the sills are found) and the uniform pressure south of 40°N. This pressure difference geostrophically balances the zonal flow that makes up the maximum of the Atlantic overturning.

We discuss now what happens when eddy coefficients are changed in the North Atlantic and Southern Ocean. Figure 8 shows the zonally averaged pressures for all SO and NA experiments for the lower layer. In all cases, the pressure value at the Equator has been subtracted. Again, the uniformity of the low latitude pressure is readily apparent in all experiments and the steep meridional mean pressure gradient between 30°N and 60°N leads to a net zonal flow of NADW that is ultimately collected into a deep western boundary current. As an integral over the lower layer, part of this flow then upwells at the boundaries and the remaining part continues southward to finally upwell in the Southern Ocean.

The lower panels of Fig. 7 show the differences in integrated pressures between the standard and SO1000 and NA1000 runs. As the pressure themselves, these differences are uniform over the Atlantic south of 40°N. For the run with changed GM coefficient in the Southern ocean, the decrease in meridional pressure gradient arises mainly from the uniform increase in low latitude pressures. For the NA1000 run, low latitude pressures decrease slightly, however the largest pressure drop occurs at high latitudes (around 50°N). As mentioned in Sect. 3, an increase in the GM coefficient in the GIN Seas decreases the density of the water there and hence also the density of the Denmark Strait overflow. Since low latitude pressures do not change significantly, pressure gradients in the South Atlantic are not changed and the South Atlantic inflow is not affected. For the SO1000 experiment, the density of the inflowing waters from the Southern ocean decreases, which leads to a decrease in low latitude pressure. Accordingly, in both SO1000 and NA1000 the maximum of the Atlantic MOC decreases compared to the standard run due to a decrease in the meridional pressure gradient, as identified from Fig. 8.

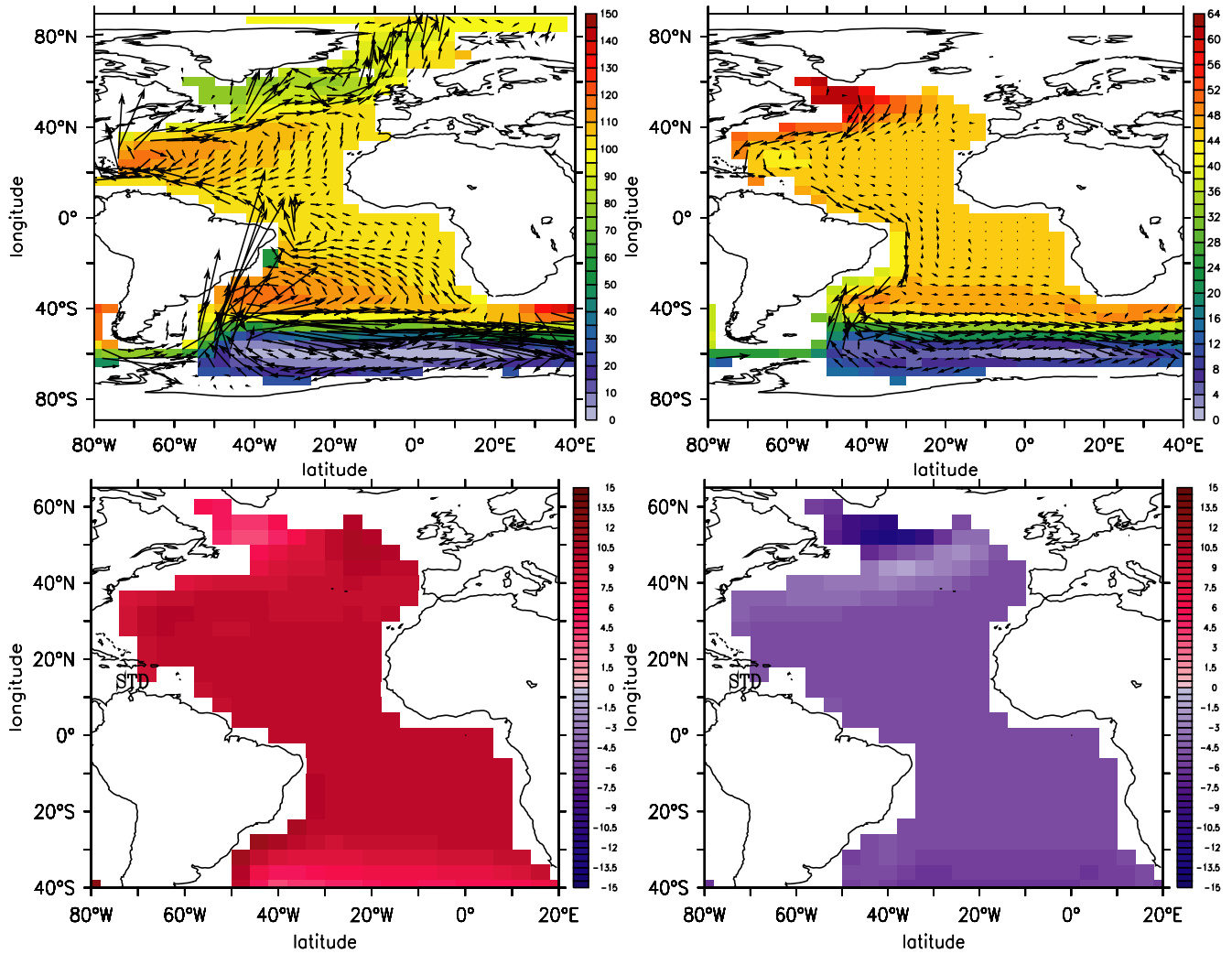
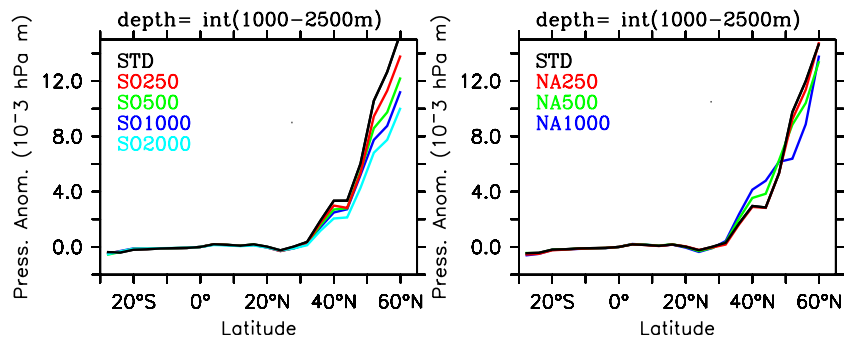


Fig. 7 Upper left Pressure (in 10^{-3} hPa m) and flow, vertically integrated between 0 and 1,000 m. Upper right Pressure (in 10^{-5} hPa m) and flow, vertically integrated between 1,000 and 2,000 m. The minimum pressure in the domain, that occurs south of

the ACC, has been subtracted. Lower panels: zoom into the Atlantic of pressure differences (in 10^{-3} hPa m) vertically integrated between 1,000 and 2,500 m. Left STD–SO1000. Right STD–NA1000

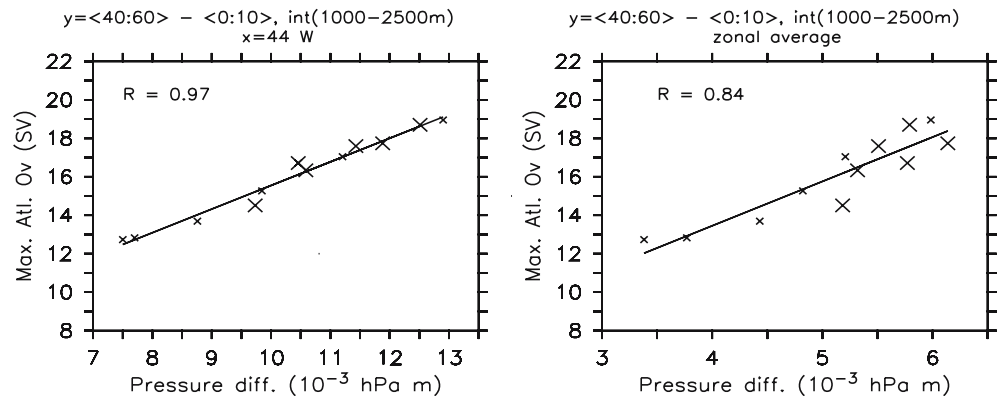
Fig. 8 Pressure vertically integrated between 1,000 and 2,500 m and zonally averaged over the Atlantic. The zonally averaged pressure at the equator in each run has been subtracted. Left SO experiments. Right NA experiments



To conclude this section, Fig. 9 shows the scatter plot of the maximum of the Atlantic MOC against the meridional pressure difference north and south of 40°N and integrated over the lower layer for all SO, NA and TROPNA experiments. As expected from the geostrophical balance at 40°N , we observe a linear

relation that is best represented by taking the pressure difference at a constant longitude of 44°W (left panel of Fig. 9). The linearity is less obvious when taking the zonally averaged integrated pressures (right panel of Fig. 9), since there is also a strong southward component of the integrated flow east of 44°W and there is a

Fig. 9 Difference of pressure averaged between 0 and 10°N and between 40 and 60°N. The pressures have been vertically integrated between 1,000 and 2,500 m. Large crosses denote NA and TROPNA experiments; small crosses denote SO experiments. *Left panel* at a constant longitude of 44°W. The linear regression coefficient is 0.97. *Right panel* zonally averaged. The linear regression coefficient is 0.84



very small local pressure minimum south of 40°S and west of 44°W (see upper left panel of Fig. 7). An interesting aspect, resulting from the uniformity of the low latitude pressure, is that there is no preference for hemispheric or interhemispheric pressure difference correlations.

4.2 Relations with pressure components at single depth levels and transient behaviour

We now discuss additional analyses for pressure components (baroclinic and barotropic) and single depth levels below and above the level of no mean motion. The following figures also include the transient states of the ‘switch-on’ experiments from year 3,800 to year 5,600 of the integrations (compare Fig. 2). The equilibrium solutions (defined as those in which the interannual variability of the Atlantic overturning components is less than 1 Sv) are displayed in purple to distinguish them from the transient states.

We start by examining the SO experiments, in which, we recall, GM diffusivities were increased only in the Southern Ocean, and determine the relations between the maximum of the Atlantic MOC and the total, baroclinic and surface pressures that hold in these simulations and for the transient states. Figure 10 shows the meridional pressure difference against the maximum overturning for the transient switch-on experiments for a depth level of 1,500 m, below the level of no mean motion (left panel), and a depth level of 500 m, above the level of no mean motion (right panel). The steady-state solution points are in purple, while all the other colors correspond to transient behaviour. The regression analysis has been done only with the steady-state points to visualize by how much the transient behaviour differs from the linear correlation of the equilibrium. The differences are taken between pressure averages at high (50°–80°N) and low (20° and 30°N) latitudes in the Atlantic Ocean. For both the high and low latitude averages, the averaging domain extends from west to east across the Atlantic and lies at a depth of 1,500 m, which is within the southward flowing core of the NADW. There is a good linear correlation for all the SO

simulations, even for the unsteady ones. When the correlation is taken at a depth of 500 m, above the level of no mean motion, the regression coefficient decreases and the transient states do not follow the linear relation as closely as for the level below the level of no mean motion (right panel of Fig. 10).

Figure 11 displays the scatter plots of the maximum of the Atlantic MOC versus the baroclinic pressure (the vertical integral of the specific weight from $z = -d$ to the surface of a resting ocean at $z = 0$) and surface pressure (surface elevation anomaly, η , times surface specific weight) differences for the SO experiments. Both pressure components added results in the scatter plot shown on the left hand side of Fig. 10. As in Fig. 10, there is a linear relation between the Atlantic MOC and the two pressure differences, although departures from linearity are obvious in the unsteady solutions. Note that the two panels are the mirror image of each other, indicating that baroclinic and surface pressure gradients have systematically opposite signs, thus partly compensating each other. The meridional surface pressure gradients are negative since the free surface elevation is higher in low latitudes, above the less dense waters, than in high latitudes above denser waters. Ultimately, for levels below the level of no mean motion, the baroclinic pressure difference dominates over the surface pressure difference, hence leading to the positive total pressure difference at 1,500 m. Interestingly, adaptations of the flow to the new equilibrium solutions are apparent in the two pressure components whereas the total pressure at 1,500 m remains on the linear correlation line. This indicates that the adaptations occur predominantly in the upper ocean, where free surface and density gradients change. Note that the total pressure distribution for single depth levels below the level of no mean motion is also uniform between 40°N and 40°S, whereas the baroclinic pressure and surface pressure distributions evidently have rich zonal and meridional structures, with local extrema at around 30°N associated with the subtropical gyre circulation (not shown).

We turn now to the experiments in which GM coefficients were changed only in the North Atlantic (NAGM). Figure 12 displays the scatter plot of the maximum of the Atlantic MOC against the hemispheric

Fig. 10 SO experiments. Differences of zonally and meridionally averaged pressures between the latitude strips 50°N–80°N and 20°N–30°N in the Atlantic. Left: at 1,500 m. Right at 500 m. Different colors refer to the different experiments with modified GM coefficients (color code is as in Fig. 5). Regression line has been calculated for equilibrium solutions (in purple)

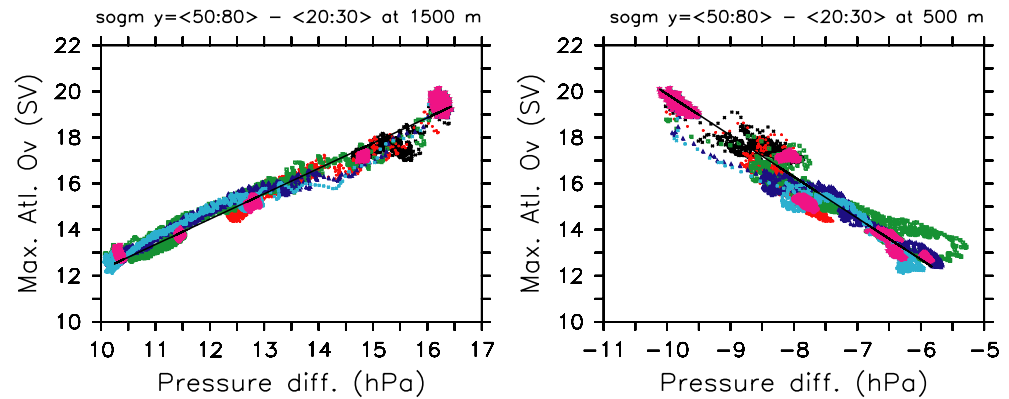
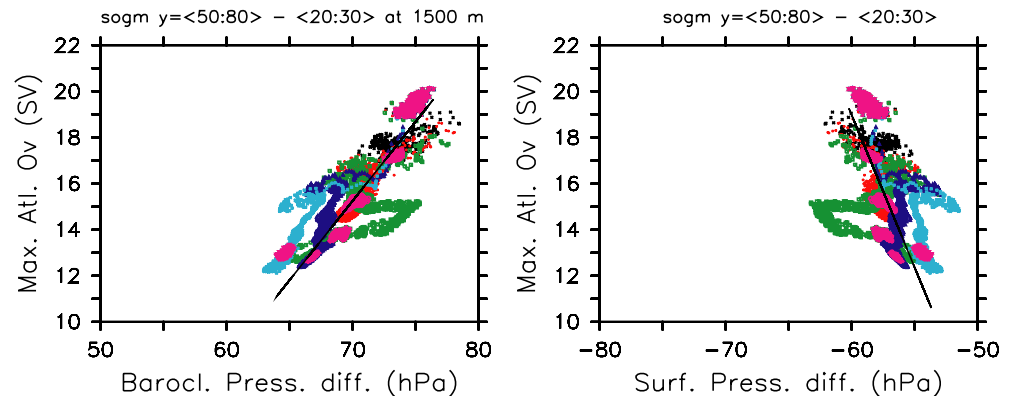


Fig. 11 SO experiments. Left Hemispheric baroclinic pressure difference at 1,500 m. Right Hemispheric surface pressure difference. Latitude strips as in Fig. 10. Color code is as in Fig. 5. Regression line has been calculated for equilibrium solutions (in purple)



pressure difference at 1,500 m. Also included is the correlation line for the same pressure difference but for the SO experiments. One notes that the unsteady solutions tend to undergo larger departures from the regression line than in the case of the SO experiments and that one of the steady-state solutions (the one for the NA1000 experiment) lies far away from the regression line. In effect, the pressure difference at 1,500 m is associated with the part of the NADW that will proceed across the Equator and flow out of the Atlantic. However, the maximum of the Atlantic MOC includes as well the recirculation caused by upwelling within the

North Atlantic at depths above 1,500 m, and this recirculation is obviously not captured by the pressure difference at 1,500 m. Clearly, the pressure difference at 1,500 m is not a diagnostic that can describe the variety of behaviour of the maximum of the Atlantic MOC and the integral over the lower layer provides a more accurate measure as described in the previous section.

In summary, linear relations are less robust for levels above the level of no mean motion and for the baroclinic and surface pressure components alone. This is particularly true for the transient states of the experiments. For the SO runs, the linear relation with the total pressure difference at single depth levels below the level of no mean motion is remarkably good even for the transient states of the switch-on experiments. This can partly be explained by the fact that in these experiments, the maximum of the Atlantic overturning is proportional to the South Atlantic outflow.

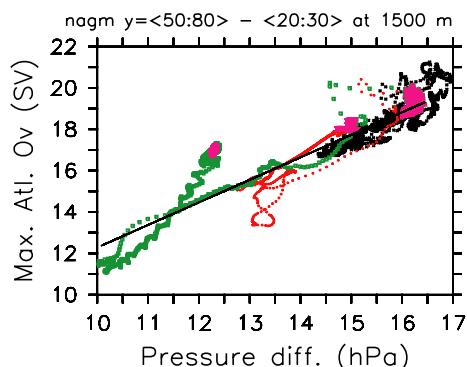


Fig. 12 Same as left panel of Fig. 10 except for NA experiments. The straight black line is the correlation line from the left panel of Figure 10. Color code is as in Fig. 5

5 The role of pressure gradients in controlling the net surface volume inflow into the Atlantic

The motivation for this section is to discuss the role of pressure gradients within the framework of the hypothesis of Nof (2003), in which, similarly to Toggweiler and Samuels (1993a), the surface volume transport from the Southern Ocean into the Atlantic is determined solely by the Southern Ocean wind stress. In

this conceptual picture, changes in pressure gradients under constant wind forcing cannot alter the South Atlantic inflow and outflow nor the maximum of the Atlantic MOC in the case when no upwelling occurs within the Atlantic. This seems somewhat in contrast to the outcome of the previous sections in which, under constant wind stress forcing, changes in the meridional pressure gradients were identified to be a crucial component.

According to Nof's (2003) theory and referring to Fig. 13, the net northward surface transport into the Atlantic at around 30°S is given by the northward interior transport minus the southward western boundary current transport. As shown by Nof (2003), the net northward transport into both the Indopacific and Atlantic across a contour passing the tips of the Americas and Africa, T_n , is formally equivalent to a wind-driven Ekman transport, and is obtained through integration along a circumpolar contour of the linearized momentum equations vertically integrated from the surface down to the depth of the sill of Drake Passage:

$$f_0 T_n = \oint \frac{\tau_x}{\rho_0} dx \quad (1)$$

From this expression, Nof (2003) obtained a net transport of around $T_n^A = 10$ Sv into the Atlantic by assuming that T_n is equi-partitioned between the Indopacific and Atlantic according to basin widths. The net northward transport in this picture is therefore solely determined by the wind. Quantitatively, it is given by the

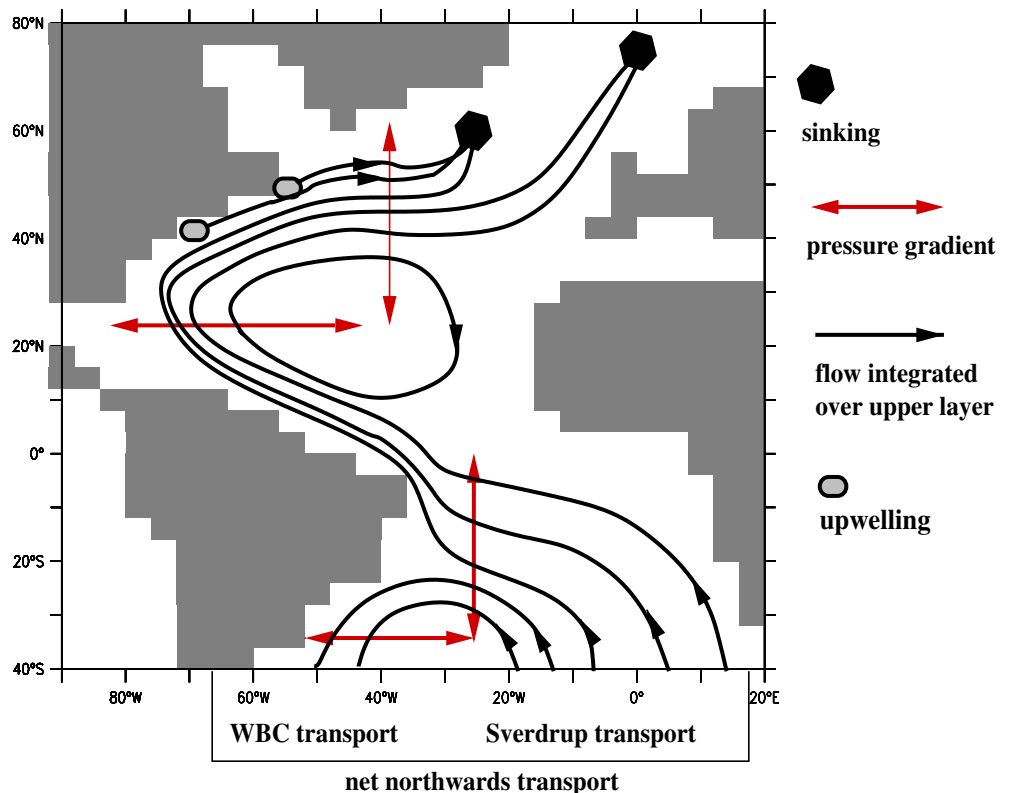
wind-driven Ekman transport from Eq. 1. However, Nof (2003) notes that the actual water mass that ultimately reaches the North Atlantic is not the water mass flowing into the Atlantic by surface Ekman transport, but the fraction of the Sverdrup transport in the ocean interior that is not flushed back out of the Atlantic via the western boundary current (Fig. 13):

$$T_n^A = \int_{x_A} \frac{1}{\beta \rho_0} \nabla \times \tau dx - \int_{x_A} \frac{1}{f \rho_0} \partial_x P_w dx \quad (2)$$

Here, x_A indicates a zonal integral across the Atlantic along a contour touching the tips of South America and Africa and τ is the wind stress along this contour. P_w is the pressure across the western boundary current. The northward flow in the ocean interior is determined by the curl of the wind stress and the transport T_n^A would be determined by the fraction of the Ekman transport from Eq. 1. Hence, the zonal pressure gradient within the western boundary current flowing along the eastern coast of South America will need to adapt in order to accommodate the return flow necessary to satisfy equation 1 and would therefore be dependent on the wind stress. Hence, the zonal and meridional pressure gradients shown as red double-headed arrows in Fig. 13 would be predetermined by the wind stress. In particular, the meridional pressure gradients analyzed in Sect. 4 would not be independent of the wind stress.

We will now assess the magnitudes of the western boundary and interior transports from Eq. 1 for the eddy experiments described in the previous sections.

Fig. 13 Sketch of surface volume transports in the Atlantic between the surface and the level of no mean motion. Drafted to qualitatively agree with the circulation depicted in the upper left panel of Fig. 7. Red arrows represent relevant pressure gradients. Also sketched are the upwelling and sinking regions within the Atlantic. The circulation pattern is consistent with that discussed by Nof (2003)



This assessment will lead us to calculate the simulated vorticity budget of the upper ocean (to examine to which extent the northward interior flow is indeed governed by Sverdrup dynamics) together with the zonal pressure gradients discussed above. The fact that the model's vertical diffusivity is very small guarantees that there is no significant upwelling within the Atlantic interior driven by diapycnal diffusion.

The vorticity balance for a general flow integrated between two levels z_1 and z_2 is (see e.g. Lu and Stammer 1998):

$$\begin{aligned} \beta V = \nabla \times & \left[-\partial_t U - \int_{z_1}^{z_2} \frac{\nabla p}{\rho_0} dz + \tau(z_1) - \tau(z_2) \right] \\ & + f[w - \mathbf{u} \cdot \nabla z_1](z_1) - f[w - \mathbf{u} \cdot \nabla z_2](z_2) \\ & + \text{LFT} + \text{ADV} \end{aligned} \quad (3)$$

Here (U, V) is the horizontal flow vertically integrated between z_1 and z_2 , and LFT and ADV are the curl of the lateral diffusion and advection, respectively. When integrated between the surface η and the ocean bottom H , $\nabla \times \int_{-H}^{\eta} \nabla p / \rho_0 dz$ is the bottom pressure torque, which is nonzero when the bottom pressure gradient is not aligned with the contours of bottom topography.

The vorticity balance for the upper layer, away from topography gradients and when lateral advection and diffusion curls can be neglected reduces thus to:

$$\beta V = \nabla \times \tau(\eta) + f w_0 \quad (4)$$

where $\tau(\eta)$ is the surface wind stress, and w_0 is the upwelling at the base of the domain of integration, which corresponds in our case to the level of no mean motion. If the upwelling is zero, the equation reduces to the familiar Sverdrup relation. Figure 14 shows the deviation from the Sverdrup balance for the standard model run with $z_1 = 0$ and $z_2 = 1,000$ m. As expected, the Sverdrup balance holds at low latitudes in the ocean interior, away from the boundaries, where deviations are well below 0.5 Sv. Vertical velocities across $z_2 = 1000$ m are large in the northernmost region of the North Atlantic, where water sinking occurs, along the path of the North Atlantic Current, and along the western boundary currents, where upwelling occurs and where friction is important. Since the vertical diffusivity in the runs is very small, there is no significant upwelling across the 1,000-m depth in the ocean interior, which would alter the balance. Note also that there is a substantial deviation from Sverdrup balance on the eastern boundary along the coasts of South Africa and Namibia.

The left panel of Fig. 15 shows the partitioning of the net northward transport at 30°S into the northward interior flow and the southward western boundary current flow for the different SO experiments. There is a deviation of the interior transport from Sverdrup balance of up to 5 Sv, which is due to a decrease in eastern boundary current inflow into the Atlantic with

increasing GM coefficient (compare also with Fig. 14 to see that Sverdrup balance is violated at the East coast of South Africa in the area of the Benguela Current). The southward western boundary current flow (the Brazil Current) increases with increasing GM coefficient for values of the GM coefficient up to about $500 \text{ m}^2 \text{ s}^{-1}$. Beyond this value, the flow seems to be virtually insensitive to further increases in the GM coefficient up to values of $2,000 \text{ m}^2 \text{ s}^{-1}$, and for even larger GM coefficients the flow decreases in unison with the interior Sverdrup flow. Clearly, in spite of the fact that the wind stress is unchanged in these experiments, the net northward transport into the Atlantic is not constant, but responds to change in the GM coefficients, which indicates that the model does not support, at least not in a strict sense, the mechanism described by Nof (2003). We now turn to examining the volume transports in the North Atlantic (right panel of Fig. 15). We recall that there is upwelling in the North Atlantic across the 1,000 m contour and that this upwelling occurs not in the ocean interior, but in the western boundary between 30°N and 50°N. The interior flow is essentially constant for all runs at around 23 Sv, while the net northward flow decreases with increasing GM coefficients until a plateau is reached for an eddy diffusivity of $1,000 \text{ m}^2 \text{ s}^{-1}$, at which stage the western boundary upwelling amounts to 5 Sv, a value that remains roughly constant for higher values of the GM coefficient.

The analysis above shows that, in our model, Nof's hypothesis does not hold in a strict sense because the net northward flow in the Atlantic ocean is not only dependent on the wind stress. Specifically, Nof's assumption that T_n^d can be calculated by partitioning T_n into contributions proportional to the widths of the Indopacific and Atlantic oceans does not hold. The net inflow from the Southern Ocean into the Atlantic is affected by changes in the zonal pressure gradients across the western and eastern boundary currents of the South Atlantic.

In the light of the analysis in Sect. 4, a note on how meridional and zonal pressure differences, as depicted in Fig. 13, are related seems appropriate. In the Southern Ocean, the indicated meridional pressure difference between the Equator, say, and the core of the subtropical gyre balances the northwestward interior flow, which is governed by Sverdrup dynamics as well as by the strength of the eastern boundary current, as discussed above. The zonal pressure difference balances the southward western boundary current. Both pressure differences are in principle independent of each other and determine together the net northward transport. For the North Atlantic, the sketched zonal pressure gradient leads to a flow one part of which ultimately sinks in the IRM and GIN Seas, while the other part recirculates in the subtropical gyre. The zonal and meridional pressure differences shown in the figure will differ by the amount needed to balance the part of the flow that upwells along the western boundary. It is therefore this meridional

Fig. 14 Deviation of the meridional flow from the Sverdrup balance ($-\nabla \times \tau / (\rho_0 \beta) - V$), with V calculated as a vertical integral from 0 to 1000 m. At each grid point, we have multiplied this deviation by the zonal grid size Δx so that the difference is given in Sv. We note that the wind stress torque (not shown) is rather noisy due to the coarse resolution of the model. Contour interval is 0.5 Sv. Positive deviations in the Southern Hemisphere mean that the meridional northward flow is larger than predicted by Sverdrup balance

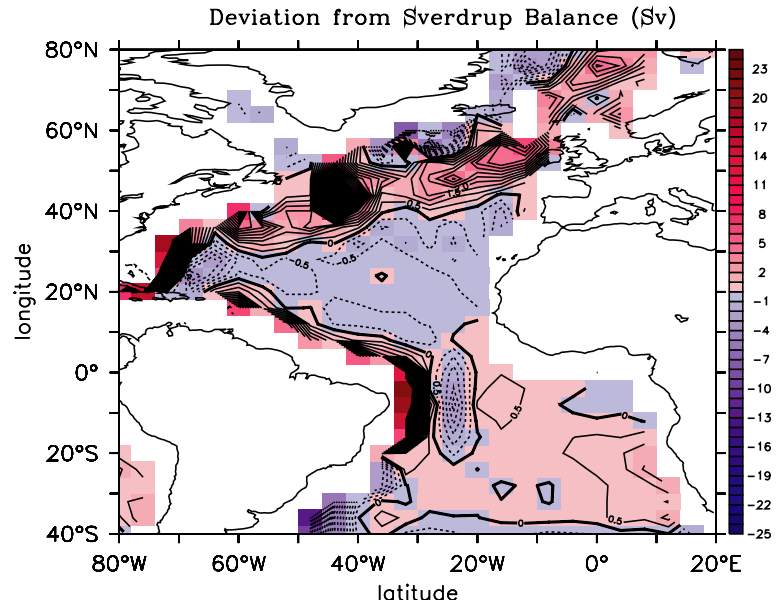
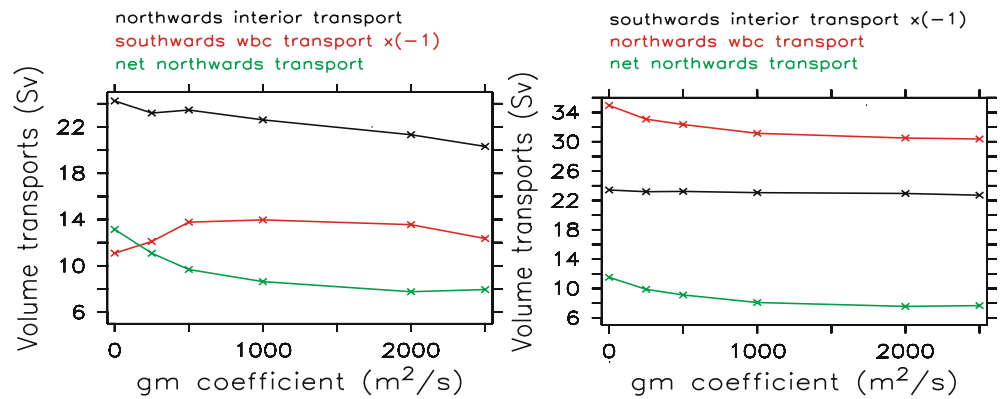


Fig. 15 *Left* northward interior transport, southward western boundary current transport and net northward transport at 30°S in the Atlantic as a function of the GM coefficient for the SO runs (the Sverdrup interior flow diagnosed from the curl of the applied wind stress is ca. 20 Sv). *Right* southward interior transport, northward western boundary current transport and net northward transport at 30°N in the Atlantic



pressure difference that determines the maximum of the Atlantic overturning, in accordance to Sect. 4.

In the next section, we will extend our analysis to experiments where changes have been introduced not only in the GM coefficients but as well in vertical diffusivities, surface freshwater forcing and wind stress, and will see that the South Atlantic outflow can vary over a range of about 10 Sv even when the wind forcing remains constant.

6 Extension to a variety of experiments

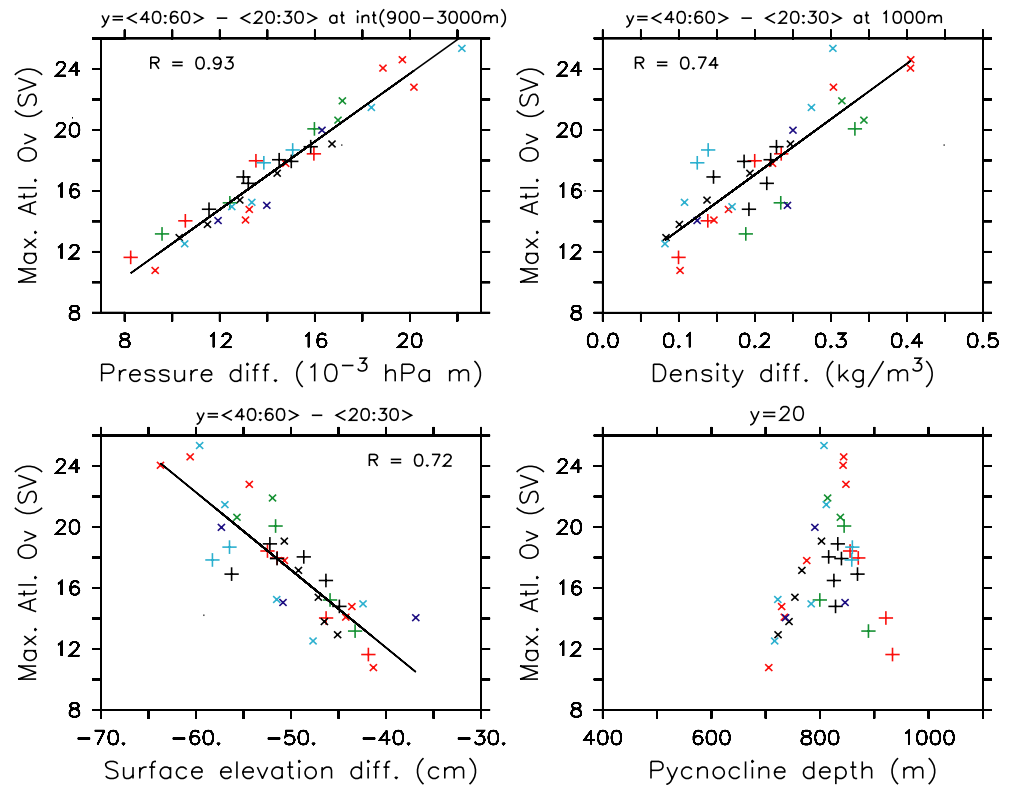
In this section we repeat the analysis of Sect. 4 but extended to a variety of experiments in which the surfaces fluxes (heat, freshwater, and winds) and the vertical diffusivities were changed as well. A summary of these experiments is given below and the color code used to display the scatter plots in Fig. 16 is indicated.

- Experiments STD, SO, NA and TROPNA discussed above (in black).

- Experiments with different surface freshwater forcing: restoring to sea surface salinity (SSS) everywhere, restoring to SSS along the coastlines only, increased river runoff (in red).
- Constant vertical background diffusivity increased to $0.3 \times 10^{-4} \text{ m}^2 \text{ s}^{-1}$, enhanced mixing at lateral boundaries and at the ocean bottom with diffusivities up to $10 \times 10^{-4} \text{ m}^2 \text{ s}^{-1}$ close to the bottom of the ocean and background diffusivity of 0.1 or $0.3 \times 10^{-4} \text{ m}^2 \text{ s}^{-1}$, Hasumi and Sugimoto (1999) (in green).
- Reduced winds: winds multiplied by 0.01 everywhere together with restoring to SSS, winds multiplied by 0.01 in the GIN Seas only, and winds multiplied by 0.01 in the Southern Ocean only (in dark blue).

Some of the above experiments were also used as baselines from which GM coefficients were again increased in the Southern Ocean and in the North Atlantic. In the experiments depicted in Fig. 16, the experiments with enhanced GM coefficients in the North Atlantic are denoted with large pluses (+) and all other experiments are denoted with small crosses (×). Here we

Fig. 16 Linear regressions between the maximum Atlantic overturning and hemispheric differences of several meridionally and vertically averaged quantities at 44°W (averaging latitude and depth ranges are indicated on top of each panel). Different colors and symbols correspond to different classes of experiments as explained in the text. SO and NA experiments from the previous sections are in black. Small crosses (x) refer to changed GM coefficients in the Southern Ocean, large plusses (+) in the North Atlantic. Upper left meridional deep pressure difference. Upper right Density difference at the level of no mean motion (for Levitus (1982), the same density difference is 0.19 kg/m³, yielding ca. 17 Sv). Lower left Surface elevation difference. Lower right pycnocline depth as diagnosed in Gnanadesikan (1999), except that it is taken at a constant latitude of 20°N and constant longitude 44°W



shall not discuss in detail the outcome of these experiments, but it is worthwhile mentioning in passing that restoring to SSSs reduces the impact of increased GM coefficients in the North Atlantic and GIN Seas on the maximum of the Atlantic MOC.

6.1 Relation of the maximum Atlantic overturning to meridional pressure and density gradients: Critique of Gnanadesikan's (1999) theory

The upper left panel of Fig. 16 shows the linear regression obtained from all the runs between the maximum of the Atlantic MOC and the meridional pressure difference integrated over the lower layer at a constant longitude (44°W), where the deep flow is directed westwards and subsequently collects into the western boundary current. The correlation between pressure difference and maximum of the Atlantic overturning is fairly high (0.93). The regression coefficient drops to 0.76 when the pressure is zonally averaged over the Atlantic (not shown). The upper right panel displays the regression with the hemispheric density difference at the level of no motion, and the lower left panel the regression with the surface elevation difference. The lower right panel shows the pycnocline depth (calculated as in Gnanadesikan (1999) but at 44°W and 20°N) against the maximum of the Atlantic MOC for all the experiments. The weakest maximum of the Atlantic MOC is 10 Sv and occurs in the experiment with restoring to SSSs only along

coastlines, a vertical diffusivity of 0.1 cm² s⁻¹, and a GM coefficient of 100 m² s⁻¹ in the Southern Ocean. The strongest overturning (26 Sv) is achieved in an experiment with very low horizontal and vertical mixing (no eddy diffusivity and a vanishing vertical diffusion coefficient).

There is a linear correlation between the maximum of the Atlantic overturning and all the different meridional measures of the flow. The correlation coefficient for the density and surface elevation difference is however much lower than for the integrated pressure difference, which is a more accurate measure of the maximum Atlantic MOC. Note that similar relations hold for the density difference at various depths and for the vertical average of the density from the level of no mean motion to the surface.

Perhaps the most revealing result displayed in Fig. 16 is that the depth of the pycnocline does not vary much from one experiment to another. The changes in the estimated depth of the pycnocline, which is calculated according to the formulation of Gnanadesikan (1999), are in the order of 100–200 m around a mean depth value of about 800 m. These pycnocline depth changes are consistent with the conceptual model of Gnanadesikan (1999) - however since the model resolution at a depth of 800 m is above 200 m, it does not resolve the possible changes in the pycnocline depth associated with the changes in diffusivities and surface forcing studied in this paper. In other words, the model pycnocline is in practice “clamped” to a depth of

around 800 m. We note that this comment is probably also valid for the original paper of Gnanadesikan (1999), who used a model with only 12 vertical levels (the vertical distribution of levels is unfortunately not provided in his paper). This is, we believe, a potentially important point, and so warrants further discussion. Gnanadesikan (1999) related the strength of the Atlantic MOC to the depth of the pycnocline, whose base defines the level of no motion, by taking into account three processes, namely, the surface Ekman flux into the Atlantic caused by Southern Ocean circumpolar winds, the return flow associated with Southern Ocean baroclinic eddies, and the upwelling of deep water at low latitudes. In the approach taken by Gnanadesikan (1999) the meridional density difference, $\Delta \rho$, is prescribed, and variations in the pycnocline depth D , leading to variations in meridional pressure gradients, control the strength of the Atlantic MOC. However, since the meridional density difference in the pycnocline does certainly change under varying ocean dynamics and surface forcing (even when restoring to surface temperatures and salinities, changes in the horizontal and vertical diffusivities, for example, will lead to variations in the density field), the meridional pressure difference (or the meridional density difference) should, in general, be treated as an independent variable in addition to the pycnocline depth. This is the path we have followed in the present work, showing that, in our model, the maximum of the Atlantic MOC appears to scale linearly with meridional pressure differences (not only above the depth of the pycnocline, but even better below) and that the pycnocline depth does not change significantly under a variety of surface forcing and ocean parameter changes. Our results are consistent with the idealized box model of Stommel (1961) and with results obtained in recent investigations reported by Levermann and Griesel (2004) and Mignot et al. (2006) using the same ocean model that we have described here. Note however that neither our results nor those of Levermann and Griesel (2004) and Mignot et al. (2006) are necessarily in contradiction with those expected from the conceptual model of Gnanadesikan (1999) (which predicts a varying pycnocline depth and a complex dependence of the maximum of Atlantic MOC on meridional pressure gradients) since the meridional density gradients are allowed to freely evolve in our simulations, while they are not in the model of Gnanadesikan (1999).

In our simulations, the pycnocline depth is close to being a constant for all experiments. The values from the lower right panel of Fig. 16 correspond to a constant velocity-gridpoint depth of ca. 876 m (Table 1). The depth of the level of no motion is located in the model level lying immediately below the pycnocline and is accordingly also constant. Since, by definition, the horizontal pressure gradient at the level of no motion is zero, the approximate pressure balance $D \Delta \rho = \Delta \eta \rho_s$ holds at the level of no motion, where the depth of the pycnocline is denoted by D , $\Delta \rho$ is the meridional density gradient vertically averaged from the surface down to

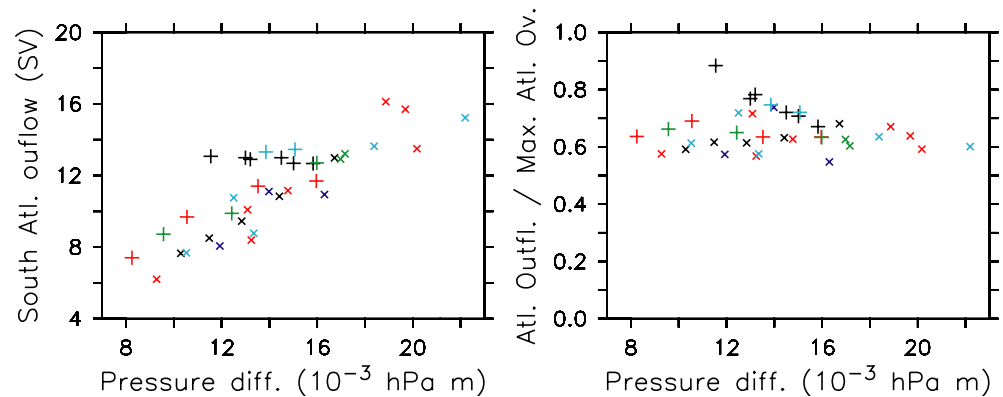
the base of the pycnocline, $\Delta \eta$ is the meridional gradient of surface elevation, and ρ_s is a reference surface density. In the sensitivity experiments run by us, changes in surface forcing and vertical and eddy mixing lead to changes in the meridional density gradient within the pycnocline which are compensated by concomitant changes in the surface elevation, so that the depth of the pycnocline remains approximately constant.

As we have pointed out above, it is unclear whether the low sensitivity of the pycnocline depth to variations in the forcing and model parameters is a genuine physical phenomenon or, rather, a model artifact related to the coarse vertical resolution. If the pycnocline behavior simulated by the model is correct, we are confronted here with the open question of what are the mechanisms and parameters that actually determine the depth of the Atlantic pycnocline, as all scaling laws so far devised predict variations of D with varying surface forcing and mixing. One possibility is that the pycnocline depth might be set by processes occurring outside the Atlantic, such as those that control the depth of the Antarctic Intermediate Water (AAIW) upon entrance in the Atlantic, at a latitude of approximately 40°S. Indeed, both the simulated and observed depth of the pycnocline coincide with the depth of the core of the AAIW at that latitude. Indeed, the experiments where the GM coefficient in the Southern Ocean is increased above 500 m² s⁻¹ are the only ones in which the depth of the AAIW core at 40°S decreases significantly and they are accompanied by an upward shift in the pycnocline depth by one level. However, it is not our purpose here to offer an alternative theory for the pycnocline, which we do not have, and we limit ourselves to just stating what we have so far observed in the model.

6.2 Relation of the South Atlantic outflow to meridional pressure gradients: critique of Nof's (2003) theory

To conclude this section, we briefly discuss as well the regression of the modelled pressure difference vertically integrated over the oceanic layer below the pycnocline with the South Atlantic outflow. Figure 17 shows such correlation for the same experiments as in Fig. 16. There is a fairly reasonable linear relation between the two quantities with the possible exclusion of the standard NA and TROPNA experiments (in which the GM coefficient is increased only in the North Atlantic and tropical Atlantic, respectively), which shows little sensitivity of the South Atlantic outflow to varying pressure differences. The range of variation of the South Atlantic outflow for all experiments is between 6 and 16 Sv, demonstrating that, in the model, the South Atlantic outflow is not exclusively controlled by Southern Ocean winds as postulated by Nof (2003). The right panel of the figure shows the ratio $R = SAO/MAXA$ which is between 0.6 and 0.8 for most experiments. The smallest ratio, below 0.6, occurs for the experiments where

Fig. 17 *Left* South Atlantic outflow as a function of interhemispheric pressure difference, integrated between 900 and 3,000 m. *Right* Interhemispheric transport efficiency $R = SAO/MAXA$. The smallest ratio is obtained for the run with the winds in the Southern Ocean multiplied by 0.01 and a vertical mixing of $0.3 \text{ cm}^2 \text{ s}^{-1}$ ($R=0.55$). The largest ratio occurs for the run with the GM coefficient set to $1,000 \text{ m}^2 \text{ s}^{-1}$ in the tropical Atlantic south of 40°N ($R=0.88$)



Southern Ocean winds are almost zero, meaning that relatively little water is exchanged between the Atlantic and the Southern Ocean. Note that the ‘small crosses’, corresponding to experiments other than those in which the GM coefficient was changed in the North Atlantic, are mostly located at a quotient of around 0.6, whereas the experiments with changed GM-coefficients in the North Atlantic exhibit ratios that can be well above 0.6.

7 Conclusions

In this paper we have investigated the effects of modifying eddy thickness diffusivities in the Southern Ocean and the North Atlantic on the distribution of large-scale density gradients in the ocean and the strength of the Atlantic MOC. Save for a few experiments discussed in Sect. 6, wind forcing is held constant in all our simulations and diapycnal mixing is ensured to be negligible.

In the model, there is a residual upwelling within the Atlantic occurring along the northern western boundary in spite of the very low diapycnal mixing rates. This upwelling decreases as higher GM coefficients are applied in the North Atlantic in the deep-water formation regions. We have also found that the values of the maximum Atlantic overturning and the South Atlantic outflow are partly independent of each other in the sense that varying the GM coefficients in the North Atlantic affects the maximum overturning but does not affect significantly the South Atlantic outflow, while changing the GM coefficients in the Southern Ocean affects both the South Atlantic outflow and the maximum Atlantic overturning by the same amount. This is due to the fact that the maximum of the Atlantic MOC is made of two contributions namely, (1) meridional recirculation in the Atlantic associated with upwelling at mid latitudes and (2) a southward outflow. Changes in the density gradients caused by alterations in the GM coefficients in the North Atlantic modify the former but not the latter contribution. Changes in the Southern Ocean affect the latter but not directly the former contribution.

We have shown as well that the maximum Atlantic MOC can be unambiguously related to a difference

between two main pressures: a high pressure south of the sills between Greenland and Scotland, where the dense sinking waters are collected, and a relatively uniform and lower pressure south of ca. 40°N . This pressure gradient creates a geostrophic zonal flow at $30\text{--}40^\circ\text{N}$ that ultimately converges onto the western Atlantic boundary and either upwells or flows southward. For experiments in which the eddy fluxes are increased in the Southern Ocean, the decrease in Atlantic overturning is mainly caused by the increase in the uniform pressure field in mid and low latitudes, whereas for experiments with increased eddy fluxes in the North Atlantic the decrease in Atlantic overturning is mainly due to the decrease in the density of the deep waters formed in the GIN Seas and the resulting decrease in the high latitude pressure. A potentially important point is that a number of authors (Thorpe et al. 2001; Rahmstorf 1996) argue in favor of an interhemispheric pressure difference. An interhemispheric density gradient has also been adopted in the box model configuration of Rooth (1982) (see also Lucarini and Stone 2005a, b) in contrast to the hemispheric set-up of the two-box Stommel model. In our model, given the uniformity of the deep Atlantic pressure field south of 40°N , there is no preference for taking a hemispheric or interhemispheric pressure difference, as both are proportional to the overturning maximum. We note, nevertheless, that the uniformity of the pressure field is only relative to the high latitudes; there are still significant zonal pressure differences south of 40°S that balance the flow in the deep western boundary current.

We can thus explain, at least partly, the diagnostic findings of previous studies with coarse resolution OGCMs, that find a linear relation between the meridional pressure difference and the Atlantic overturning maximum. We have shown that this linear relation holds for a large variety of experiments, including changes in surface freshwater and wind forcing and in subgridscale parameterizations of isopycnal and diapycnal mixing.

The analyses of the linear relation with the meridional pressure difference for the transient states of the experiments have revealed a remarkably good correlation for the SO experiments. This might be promising for

a possible diagnosis of changes in the Atlantic overturning from meridional density or pressure gradient time series in the real ocean. It seems particularly interesting that the baroclinic and surface pressure components show more of a variability in the adaptation process, leading one to conclude that it is the upper ocean properties that non-linearly adapt to a new strength of the Atlantic overturning circulation. The relevance of timescales of the Atlantic overturning circulation and the difference between transient and stationary states has been discussed by e.g. Lucarini and Stone (2005a, b) and Lucarini et al. (2005) but note that the emphasis here was not to investigate in detail how the adaptation to the new equilibrium states is achieved and which timescales are involved and must be left for future work.

Our results suggest that the ansatz of Gnanadesikan (1999) is not satisfied by our model, since the pycnocline depth changes associated with the different processes discussed by Gnanadesikan (1999) are not resolved in the model owing to its very coarse vertical resolution. In the model, it is not the level of no motion or the pycnocline depth that changes as a result of changes in the forcing or the mixing, but the meridional density difference, and hence the surface elevation and meridional pressure difference. Our model behaviour is closer to that of the box model of Stommel (1961), in which the vertical scales of the boxes are prescribed, while the meridional density difference is allowed to change and hence determines the flow. Whether experiments with an increased vertical resolution will confirm this hypothesis of ours is left for future work. From our model simulations, we conclude that any variation in Atlantic overturning, be it through increased eddy fluxes, of changed wind stress, vertical mixing or surface fresh water fluxes, can diagnostically be related to the change in meridional pressure difference. This illustrates once more the important interaction between the thermohaline and wind-driven components of the meridional circulation, since also in the experiments where only the wind stress was changed, pressure gradients adapted in such a way that the linear relation between meridional pressure gradients and maximum of the Atlantic MOC was maintained.

In Sect. 5, we have attempted to link the picture of a wind driven Atlantic overturning (Nof 2003) to changes in the density gradients that occur in the North Atlantic and Southern Ocean when the GM coefficients are modified. We have argued that, for the South Atlantic outflow, the pressure gradients influencing the southward western boundary current and northward eastern boundary current do indeed influence the net inflow into the Atlantic, which can vary significantly even if the wind stress remains constant. The analysis was extended to a variety of experiments. With the exception of two experiments in which the Southern ocean wind stress was reduced, all the simulations used the same wind forcing. Nevertheless, the South Atlantic outflow was shown to vary over a range of 10 Sv for the different experiments. The net northward

meridional volume transport into all ocean basins across a closed latitude circle at, say, 60°N is solely wind determined. However, the volume of waters that ultimately reaches the North Atlantic depends on the distribution of pressure gradients along the paths of the northward traveling water masses. In our model, a purely wind-driven circulation can be realized in which Southern Ocean wind stress and not diapycnal mixing provides the main energy source for the upwelling of NADW. However, the actual strength of the maximum Atlantic MOC is not uniquely determined by the Southern Ocean wind stress but also by the density/pressure gradients in the deep-water formation regions as well as in the Southern Ocean.

This aspect seems particularly important considering the consequences for stability of the Atlantic MOC. In an ocean where the overturning circulation would be mainly determined by Southern Ocean westerlies, deep water formation in the North Atlantic would play a more passive role. If on the other hand, pressure gradients within the outflow region in the Southern Ocean can vary over a broad range independently of the Southern Ocean wind-stress, deep water formation in the North Atlantic is allowed to vary more independently and also a stable off-state can exist. It has been suggested by (Nof 2000; DeBoer and Nof 2004, 2005) that the opening or closing of the Bering Strait gap has important consequences for the Atlantic overturning circulation. Rather than integrating over a closed circle in the Southern Ocean, they integrate over a closed loop passing along the eastern boundary of the Atlantic ocean all the way across the Arctic, through the Bering Strait and along the Western Pacific coast back across the South Atlantic ocean. In their argument, subject to a number of assumptions and requiring continuity across Bering Strait, the net pressure gradient along such a loop would also vanish, leaving again the Southern Ocean windstress as the main player for the Atlantic overturning circulation. DeBoer and Nof (2004) argue that a closed Bering Strait configuration on the other hand exhibits less stable conditions. We have conducted additional experiments with an open Bering Strait and find that the Atlantic overturning circulation is very sensitive to the additional freshwater input from the Pacific to the Arctic. The experiment with open Bering Strait and increase of the eddy diffusion coefficient by $1,000 \text{ m}^2 \text{ s}^{-1}$ in the Southern Ocean yields a maximum and South Atlantic outflow of the Atlantic overturning circulation of only 4 Sv. The experiment with the strongest Atlantic overturning of the experiments discussed in Sect. 6 (MAXA = 26 Sv, SAO = 15 Sv) also has a reduced Atlantic overturning with open Bering Strait (MAXA = 20 Sv, SAO = 12 Sv). Overall, these experiments seem to further indicate that it is not the Southern Ocean winds that exert the only control on the Atlantic overturning circulation.

For understanding the behaviour of the maximum of the Atlantic MOC, taking the upwelling that occurs along the western boundary into account is crucial. In all our experiments, including the ones with an increased vertical mixing coefficient of $0.3 \text{ cm}^2 \text{ s}^{-1}$, there is no significant upwelling within the Atlantic ocean interior, and the

dominant upwelling takes place along the Atlantic western boundary. There are therefore no deep horizontal recirculations in our model, in contrast to the original Stommel and Arons (1960) framework, which could further alter the modelled meridional and zonal pressure gradient relations.

Acknowledgements We are grateful to Marisa Montoya, Anders Levermann, Andrey Ganopolski, Stefan Rahmstorf, Matthias Hofmann, Till Kuhlbrodt, Eva Bauer and Juliette Mignot for useful discussions. The comments of 2 reviewers are greatly appreciated. A.G. was funded through the James S. McDonnell Foundation Centennial Fellowship.

References

- Berliand M, Berliand T (1952) Measurements of the effective radiation of the earth with varying cloud amounts. *Izv Akad Nauk SSR, Ser Geofiz*, p 1
- Böning C, Holland W, Bryan F, Danabasoglu G, McWilliams J (1995) An overlooked problem in model simulations of the thermohaline circulation and heat transport in the Atlantic ocean. *J Clim* 8:515–523
- DeBoer A, Nof D (2004) The Bering Strait's grip on the northern hemisphere climate. *Deep Sea Res* 51:1347–1366
- DeBoer A, Nof D (2005) The island wind-buoyancy connection. *Tellus* 57A:783–797
- Fichefet T, Maqueda MM (1997) Sensitivity of a global sea ice model to the treatment of ice thermodynamics and dynamics. *J Geophys Res* 102:12609–12646
- Gent P, McWilliams J (1990) Isopycnal mixing in ocean circulation models. *J Phys Oceanogr* 20:150–155
- Gnanadesikan A (1999) A simple predictive model for the structure of the oceanic pycnocline. *Science* 283:2077–2079
- Griffies S (1997) The Gent–McWilliams skew flux. *J Phys Oceanogr* 28:831–841
- Hasumi H, Suginozono N (1999) Effects of locally enhanced vertical diffusivity over rough bathymetry on the world ocean circulation. *J Geophys Res* 104:23367–23374
- Hofmann M, Morales-Maqueda M (2006) Performance of a second-order moments advection scheme in an ocean general circulation model. *J Geophys Res* (accepted)
- Huang R (1999) Mixing and energetics of the oceanic thermohaline circulation. *J Phys Oceanogr* 29:727–746
- Huck T, de Verdiere AC, Weaver A (1998) Interdecadal variability of the thermohaline circulation in box-ocean models forced by fixed surface fluxes. *J Phys Oceanogr* 29:865–892
- Kalnay E, Kanamitsu M, Kistler R, Collins W, Deaven D, Gandin L, Iredell M, Saha S, White G, Woollen J, Zhu Y, Chelliah M, Ebisuzaki W, Higgins W, Janowiak J, Mo K, Ropelewski C, Wang J, Leetmaa W, Reynolds R, Jenne R, Joseph D (1996) The NCEP/NCAR 40-year reanalysis project. *Bull Am Meteor Soc* 77:437–471
- Kamenkovich I, Sarachik E (2004) Mechanisms controlling the sensitivity of the Atlantic thermohaline circulation to the parameterization of eddy transports in ocean GCMs. *J Phys Oceanogr* 34:1628
- Large W, Pond S (1981) Open ocean momentum flux measurements in moderate to strong winds. *J Phys Oceanogr* 11:324–336
- Large W, Pond S (1982) Sensible and latent heat flux measurements over the ocean. *J Phys Oceanogr* 12:464–482
- Lazar A, Madec G, Delecluse P (1999) The deep interior downwelling, the Veronis effect, and mesoscale tracer transport parameterizations in an OGCM. *J Phys Oceanogr* 29:2945–2961
- Levermann A, Griesel A (2004) Solution of a model for the oceanic pycnocline depth: Scaling of overturning strength and meridional pressure difference. *Geophys Res Lett* 31
- Levitus S (1982) Climatological atlas of the world ocean. NOAA Prof Pap 13:173
- Lu Y, Stammer D (1998) Vorticity balance in coarse-resolution global ocean simulations. The ECCO Report Series 15
- Lucarini V, Stone P (2005a) Thermohaline circulation stability: a box model study. part I: uncoupled model. *J Clim* 18:501–513
- Lucarini V, Stone P (2005b) Thermohaline Circulation stability: a box model study. Part II: coupled atmosphere-ocean model. *J Clim* 18:514–529
- Lucarini V, Calmanti S, Artale V (2005) Destabilization of the thermohaline circulation by transient changes in the hydrological cycle. *Clim Dyn* 24:253–262
- Mignot J, Levermann A, Griesel A (2006) A decomposition of the Atlantic meridional overturning circulation into simple physical processes using its sensitivity to vertical mixing. *J Phys Oceanogr* (in press)
- Munk W, Wunsch C (1998) Abyssal recipes II: energetics of tidal and wind mixing. *Deep Sea Res* 45:1977–2010
- National Geophysical Data Center (1988) Data Announcement 88-MGG-02, Digital relief of the surface of the Earth, National Oceanic and Atmospheric Administration (NOAA), Boulder
- Nof D (2000) Does the wind control the import and export of the South Atlantic?. *J Phys Oceanogr* 30:2650–2667
- Nof D (2003) The Southern Ocean's grip on the northward meridional flow. *Prog Oceanogr* 56:223–247
- Pacanowski R, Griffies S (1999) The MOM-3 manual. GFDL Ocean Group, NOAA/Geophysical Fluid Dynamics Laboratory, Princeton
- Parkinson C, Washington W (1979) A large-scale numerical model of sea ice. *J Geophys Res* 84:311–337
- Prather M (1986) Numerical advection by conservation of second-order moments. *J Geophys Res* 91:6671–6681
- Rahmstorf S (1996) On the freshwater forcing and transport of the Atlantic thermohaline circulation. *Clim Dyn* 12:799–811
- Rooth C (1982) Hydrology and ocean circulation. *Prog Oceanogr* 11:131–149
- Shine K (1984) Parameterization of shortwave flux over high albedo surfaces as a function of cloud thickness and surface albedo. *Q J R Meteorol Soc* 110:747–764
- Stommel H (1961) Thermohaline convection with two stable regimes of flow. *Tellus* 13:224–230
- Stommel H, Arons A (1960) On the abyssal circulation of the world ocean—I. Stationary planetary flow patterns on a sphere. *Deep Sea Res* 6:151–173
- Thorpe R, Gregory J, Johns T, Wood R, Mitchell J (2001) Mechanisms determining the Atlantic thermohaline circulation response to greenhouse gas forcing in a non-flux-adjusted coupled climate model. *J Clim* 14:3102–3116
- Toggweiler J, Samuels B (1993a) Is the magnitude of the deep outflow from the Atlantic ocean actually governed by southern hemisphere winds? In: Heimann M (ed) *Global carbon cycle*, NATO ASI Series, Springer, Berlin Heidelberg New York, pp 333–366
- Toggweiler J, Samuels B (1995) Effect of Drake passage on the global thermohaline circulation. *Deep Sea Res* 42:477–500
- Toggweiler J, Samuels B (1998) On the ocean's large-scale circulation near the limit of no vertical mixing. *J Phys Oceanogr* 28:1832–1852
- Veronis G (1975) The role of models in tracer studies. Numerical models of ocean circulation. *Natl Acad Sci* 133–146
- Wright D, Stocker T, Mercer D (1997) Closures used in zonally averaged ocean models. *J Phys Oceanogr* 28:791–804
- Wunsch C, Ferrari R (2004) Vertical mixing, energy and the general circulation of the oceans. *Annu Rev Fluid Mech* 36:281–314
- Yang J (2003) On the importance of resolving the western boundary layer in wind-driven ocean general circulation models. *Ocean Modell* 5:357–379
- Zillmann J (1972) A study of some aspects of the radiation and the heat budgets of the southern hemisphere oceans. *Meteor Stud* 26:562. Bur. of Meteorology, Department of the Interior, Canberra